Available online at www.sciencedirect.com
SCIENCE DIRECT®
Journal of Nuclear Materials 324 (2004) 90–96
journal of nuclear materials
www.elsevier.com/locate/jnucmat

Modelling of copper precipitation in iron during thermal aging and irradiation

F. Christien *, A. Barbu

Laboratoire des Solides Irradiés, CEA/DSM/DRECAM, Ecole Polytechnique, 91128 Palaiseau cedex, France

Received 15 May 2003; accepted 26 August 2003

Abstract

The cluster dynamics model for precipitation (CD-P model) described in [J. Nucl. Mater. 245 (1997) 224] has been improved and applied to copper precipitation in Fe–Cu and Fe–Cu–Ni during thermal aging at different temperatures. The CD-P model was tested on atom probe measurements [Mater. Sci. Eng. A 250 (1998) 49] and small angle neutron scattering (SANS) measurements [J. Nucl. Mater. 245 (1997) 224; Springer Proc. Phys. 10 (1986) 73]. Copper diffusivity was found to be a little higher than that proposed by Salje and Feller-Kniepmeier [J. Appl. Phys. 48 (1977) 1833]. The binding energy proposed in [J. Nucl. Mater. 277 (2000) 113] was also tested and it was concluded that little change occurs compared to the classical capillary model. Assuming a constant vacancy concentration (in other words a constant Cu diffusivity), the CD-P model was then applied to electron and neutron irradiation at 290 °C. In a second step, the CD-P model and the cluster dynamics model for vacancy and interstitial clustering (CD-VIC model) described in [J. Nucl. Mater. 302 (2002) 143] were mixed so as to really describe precipitation under irradiation by taking into account the evolution of vacancy concentration with time. The result is that the agreement between modelling and experimental data is better, specially in the case of neutron irradiation.

PACS: 61.72.−y; 61.72.Ji; 66.30.Fq

1. Introduction

Embrittlement of the pressure vessels steels during thermal aging or irradiation is partly due to copper precipitation. That is why models were proposed in the recent years to describe homogeneous precipitation. In the past, the cluster dynamics model for precipitation (CD-P model) (see [1] for detailed description) was not always successfully applied, specially due to the uncertainty on copper diffusivity data and on certain experimental data.

In the first part of this work, the results of the CD-P model are compared to experimental data of *thermal aging*, regarding copper diffusivity as a fitting parameter. The following parts deal with the modelling of copper precipitation during *electron* and *neutron irradiation*.

2. Copper precipitation during thermal aging

The temperature dependence of the copper solubility in iron alloys is given by

$$C_{\mathrm{eq}}(T) = \exp\left(\frac{\Delta S}{k}\right)\exp\left(-\frac{\Omega}{kT}\right), \tag{1}$$

where C_{eq} is the copper solubility, ΔS is a non-configurational entropy term, Ω is the demixing energy, k the Boltzman's constant and T the absolute temperature.

* Corresponding author. Tel.: +33-1 69 08 29 32; fax: +33-1 69 08 68 67.
E-mail address: fchristien@cea.fr (F. Christien).

0022-3115/$ - see front matter © 2003 Elsevier Ltd. All rights reserved.
doi:10.1016/j.jnucmat.2003.08.035

2.1. Fe–1.1at.%Cu–1.4%Ni alloy

In a previous work, Miller studied copper precipitation in a Fe–1.1at.%Cu–1.4%Ni alloy by atom probe field ion microscopy [2]. In that work, the copper content in the matrix was measured after long time aging at different temperatures. Since the equilibrium was reached at several temperatures, $\Delta S/k$ and Ω/k could be determined:

$$\begin{aligned} \Omega/k &= 6255 \text{ K}, \\ \Delta S/k &= 0.866. \end{aligned} \tag{2}$$

The CD-P model was applied at 300, 400 and 500 °C and the copper diffusivity was adjusted each time so as to fit the experimental data (Fig. 1). These adjusted copper diffusion coefficients were reported against temperature in an Arrhenius diagram (Fig. 2) and the temperature dependence of copper diffusivity D_{Cu} was deduced (Eq. (3)). It is a little higher than the diffusivity of copper in iron proposed by Salje and Feller-Kniepmeier [4].

$$D_{Cu}(T) = 0.63 \exp\left(-\frac{2.29 \text{ eV}}{kT}\right) \text{ cm}^2\,\text{s}^{-1}. \tag{3}$$

According to [2], the initial matrix copper content (0.91 at.%Cu) is lower than the nominal content because of inhomogeneous precipitation at dislocations and grain boundaries during prior annealing at 850 °C. So, the copper matrix content that we considered in our calculations is 0.91 at.%.

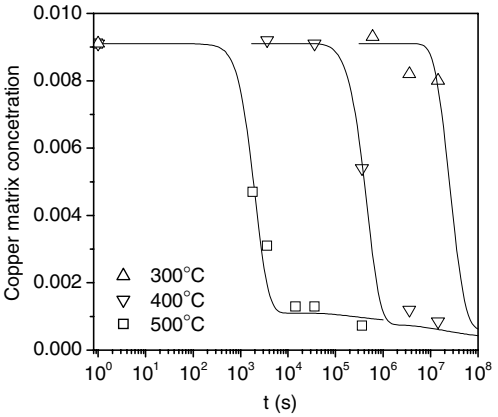

Fig. 1. Evolution of the copper matrix content during thermal aging of the Fe–1.1at.%Cu–1.4%Ni alloy. The points correspond to the experimental values measured by atom probe microscopy [2] and the curves were calculated by the CD-P model.

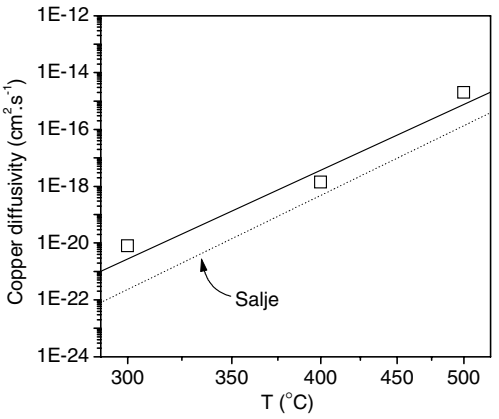

Fig. 2. Copper diffusivity in the Fe–1.1at.%Cu–1.4%Ni alloy.

2.2. Fe–1.34at.%Cu alloy

Mathon et al. [1] and Kampmann and Wagner [3] studied copper precipitation in a Fe–1.34at.%Cu alloy during thermal aging at 500 °C. They measured by small angle neutron scattering (SANS) the evolution of mean cluster radius and cluster density with time (Fig. 3).

The CD-P model was applied using the parameters given in Eq. (2) and adjusting the copper diffusivity to get the best fit. Only the clusters containing more than 10 copper atoms were taken into account for the calculation of the mean radius and the cluster density. A quite good agreement was found between the model and the experimental data (Fig. 3). The copper diffusivity used in the fit is 7.7×10^{-15} cm^2 s^{-1}, which is very close to the value found for the Fe–1.1at.%Cu–1.4%Ni alloy at 500 °C (2.0×10^{-15} cm^2 s^{-1}).

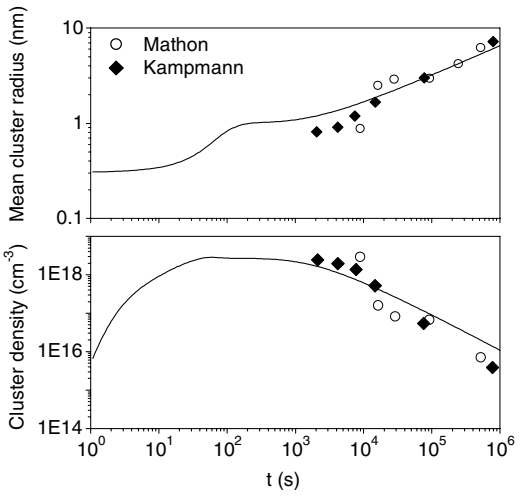

Fig. 3. Evolution of the mean cluster radius and the cluster density during thermal aging at 500 °C. The points correspond to the experimental values measured by SANS [1,3] and the curves were calculated by the CD-P model.

It must be noticed that not all the experimental points by Kampmann are shown in Fig. 3. Kampmann also measured the mean cluster radius and the cluster density after very short aging times at 500 °C: 300 and 1000 s (see [3]). The mean radii measured for these short aging times were about 0.5 nm, which is twice smaller than predicted by the CD-P model (see Fig. 3). Nevertheless, this difference (≈0.5 nm) is not very large compared to the sensitivity of the SANS technique.

Moreover, it seems to us that for aging times as short as 300 or 1000 s, the heating time needed to reach the target temperature (here 500 °C) cannot be neglected any longer and should be taken into account in the model, which was not done here. Although nothing is said in [3] about how the aging treatments were made at 500 °C, it can be supposed that the samples were aged in a resistively heated vacuum furnace in which the heating rate is rather low. For example, it takes approximately 2000 s to reach 500 °C in Mathon's work. Assuming that heating rate is of the same order of magnitude in Kampmann's work, the heating time cannot be neglected compared to aging times of 300 and 1000 s.

2.3. Comments about the validity of the capillary model

The CD-P model used here is based on the classical capillary model in which the binding energy E_B of a cluster containing n atoms is given by

$$E_B = \Omega - T\Delta S - (36\pi)^{1/3} V_{at}^{2/3} \sigma \left(n^{2/3} - (n-1)^{2/3} \right), \quad (4)$$

where V_{at} is the atomic volume and σ is the cluster–matrix interface energy calculated using the Cahn–Hilliard model [1,7]. Eq. (4) is plotted in Fig. 4.

Golubov et al. [5] proposed to use another binding energy instead of the one given by Eq. (4). This binding energy is shown in Fig. 4. The CD-P model was tested for the Fe–1.34at.%Cu at 500 °C with the two binding energies: the one given by the classical capillary model (Eq. (4)) and the one proposed by Golubov (Fig. 4). In order to compare the results obtained by the CD-P model for the two binding energies shown in Fig. 4, we used the same copper diffusivity in both cases. This diffusivity is the one used by Golubov et al. in [5] and is given by Eq. (5) [8,9]:

$$D_{Cu}(T) = 7.08 \exp\left(-\frac{2.53 \text{ eV}}{kT} \right) \text{cm}^2\,\text{s}^{-1}. \quad (5)$$

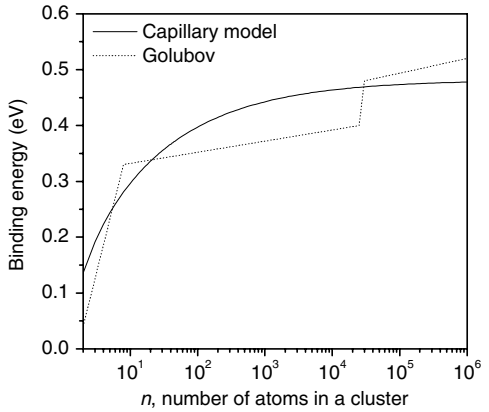

Fig. 4. Binding energy of the copper clusters. Comparison between the capillary model and the function proposed by Golubov et al. in [5].

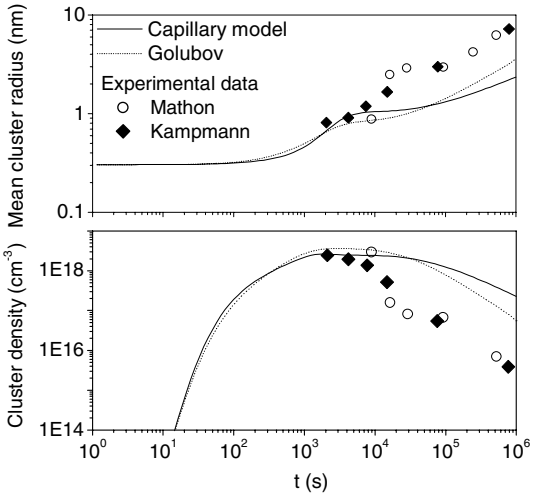

Fig. 5. Evolution of the mean cluster radius and the cluster density during thermal aging at 500 °C calculated by the CD-P model using two different binding energies: the one given by the classical capillary model and the one proposed by Golubov et al. in [5]. In both cases, we used the same diffusivity as in [5].

The results are shown in Fig. 5. Mathon's and Kampmann's experimental data were also reported in Fig. 5. It can be seen from Fig. 5 that in the present case the capillary model and the binding energy proposed by Golubov lead to almost identical results. The binding energy proposed by Golubov does not enable either to fit the experimental data, as already found in [5].

It is our opinion that the calculations shown in Fig. 5 do not fit the experimental data because the copper diffusivity deduced from Eq. (5) is simply too low. Many other shapes of the binding energy function were tested in this work and it was never possible to fit the experimental data using the diffusivity deduced from Eq. (5).

3. Copper precipitation during electron irradiation

Electron irradiations (2.5 MeV) were performed by Mathon on the Fe–1.34at.%Cu alloy at 290 °C [1]. The

dose rate was 6×10^{-6} C cm^{-2} s^{-1}, which corresponds to a point defect production rate of 2×10^{-9} dpa s^{-1}.

The evolution with time of mean cluster radius and cluster density were then measured by SANS. To apply the CD-P model in this case, one must consider the effective copper diffusivity taking into account the vacancy concentration in the alloy under irradiation. This vacancy concentration can be estimated in the permanent regime by taking into account the point defect production rate, the recombination rate of vacancies with self-interstitial atoms (SIA) and the elimination of vacancies on dislocations. Considering a dislocation density of 10^8 cm^{-2}, it can be shown that the effect of grain boundaries on the elimination of vacancies is negligible compared to the effect of dislocation density, because of a rather large grain size (≈30 μm). Neglecting the vacancy and SIA concentration values at equilibrium, the evolution of the vacancy and SIA concentrations with time is given by the following differential equation system:

$$\begin{cases} \frac{\partial C_v}{\partial t} = G_v - k_{iv}C_iC_v - D_vC_v\rho_d, \\ \frac{\partial C_i}{\partial t} = G_i - k_{iv}C_iC_v - z_iD_iC_i\rho_d, \end{cases} \tag{6}$$

where $C_v(C_i)$ is the vacancy (SIA) concentration, $G_v(G_i)$ is the vacancy (SIA) production rate ($G_v = G_i = G$), k_{iv} is the recombination rate between vacancies and SIA, $D_v(D_i)$ is the vacancy (SIA) diffusion coefficient, ρ_d is dislocation density and z_i is the dislocation bias towards SIA. k_{iv} is given by

$$k_{iv} = \frac{4\pi}{V_{at}} r_{iv}(D_i + D_v) \approx \frac{4\pi}{V_{at}} r_{iv}D_i, \tag{7}$$

where r_{iv} is the recombination radius. For iron, $r_{iv} \approx 6.5$ Å.

In the permanent regime, $\partial C_v/\partial t = \partial C_i/\partial t = 0$ and solving Eqs. (6) leads to

$$C_v = -\frac{\rho_d z_i D_i}{2k_{iv}} + \left(\left(\frac{\rho_d z_i D_i}{2k_{iv}} \right)^2 + \frac{G z_i D_i}{k_{iv} D_v} \right)^{1/2}. \tag{8}$$

For the Fe–1.34at.%Cu at 290 °C, we have, according to [6]: $\rho_d = 10^8$ cm^{-2}, $D_i = 8.3\times10^{-7}$ cm^2 s^{-1} and $D_v = 2.4\times10^{-12}$ cm^2 s^{-1}. The electron irradiations were performed with a point defect production rate of 2×10^{-9} dpa s^{-1}. The dislocation bias towards SIA is $z_i = 1.2$ [6]. We finally get: $C_v = 1.2\times10^{-7}$.

The copper diffusivity D^{irr} under irradiation can be calculated from

$$D^{irr} = D^{th}\frac{C_v}{C_v^{eq}}, \tag{9}$$

where D^{th} is the copper thermal diffusivity and C_v^{eq} is the vacancy concentration at equilibrium. D^{th} was determined using Eq. (3). The vacancy formation energy E_v^f is 1.6 eV in iron, which corresponds to an equilibrium vacancy concentration $C_v^{eq} = 4.9\times10^{-15}$ at 290 °C. Thus, copper diffusivity under irradiation at 290 °C is $D^{irr} = 5.5\times10^{-14}$ cm^2 s^{-1}.

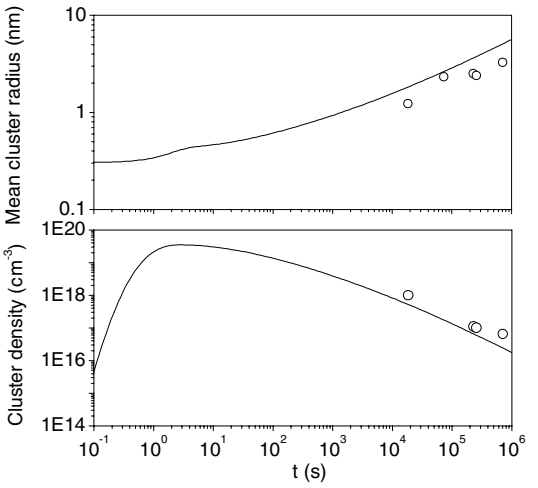

Fig. 6. Evolution of the mean cluster radius and the cluster density during electron irradiation at 290 °C. The CD-P model was applied assuming a constant vacancy concentration.

The CD-P model was applied using this copper diffusivity value and the thermodynamic parameters of Eq. (2). The results were compared to Mathon's experimental data (Fig. 6) and a quite good agreement can be observed.

Table 1
Parameters introduced in the CD-P-VIC model for point defect clustering under electron irradiation

	Symbol	Value
Point defect production rate	G	2×10^{-9} dpa s^{-1}
Temperature	T	290 °C
Grain size	d	30 μm
Vacancy formation energy	E_v^f	1.6 eV
SIA formation energy	E_i^f	4.3 eV
Vacancy migration energy	E_v^m	1.3 eV
SIA migration energy	E_i^m	0.3 eV
Pre-exponential factor of vacancy diffusivity	D_{v0}	1 cm^2 s^{-1}
Pre-exponential factor of SIA diffusivity	D_{i0}	4×10^{-4} cm^2 s^{-1}
Recombination radius	r_{iv}	6.5 Å
Dislocation density	ρ_d	10^8 cm^{-2}
Capture efficiency of vacancies by dislocations	z_v	1.0
Capture efficiency of SIA by dislocations	z_i	1.2
Di-vacancy binding energy	E_{2v}^B	0.8 eV
Di-interstitial binding energy	E_{2i}^B	1.2 eV

The vacancy concentration calculated using Eq. (8) is only an approximation since it is true only in the permanent regime and moreover, point defect clustering is neglected. That is why the above CD-P model was mixed with the cluster dynamics model for vacancy and interstitial clustering (CD-VIC model) presented in [6] in order to take into account the evolution of the vacancy concentration with time during irradiation. In the following, this 'mixed' model will be called the cluster dynamics model for precipitation and vacancy and interstitial clustering (CD-P-VIC model). In this model, the mobility of the small point defect clusters is considered following the simple law:

$$D(n) = \frac{D(1)}{n}, \tag{10}$$

where $D(n)$ is the diffusivity of a cluster of size n (i.e. containing n point defects) and $D(1)$ the diffusivity of the point defect. For $n > 40$, we take: $D(n) = 0$.

Copper diffusivity can be calculated at each time step in the CD-P-VIC model according to Eq. (9). Copper thermal diffusivity at 290 °C was calculated using Eq. (3) and the thermodynamic parameters given by Eq. (2) were used for copper precipitation. The others data introduced in the model concern point defect clustering and are summarised in Table 1. These data are the same as in [6], except the di-vacancy binding energy ($E^{B}_{2v} = 0.2$ eV in [6]). The reason why we chose $E^{B}_{2v} = 0.8$ eV in this study is discussed in [10].

The results are shown in Fig. 7. The results obtained by the CD-P model assuming a constant vacancy concentration (Fig. 6) were also reported in Fig. 7. It can be observed that the results of both models (CD-P model and CD-P-VIC model) are very close to each other in the coarsening regime where the experimental data lie. Nevertheless, nucleation and copper matrix depletion are much slower according to the CD-P-VIC model. This is easily understandable according to the evolution of the vacancy concentration with time (Fig. 7).

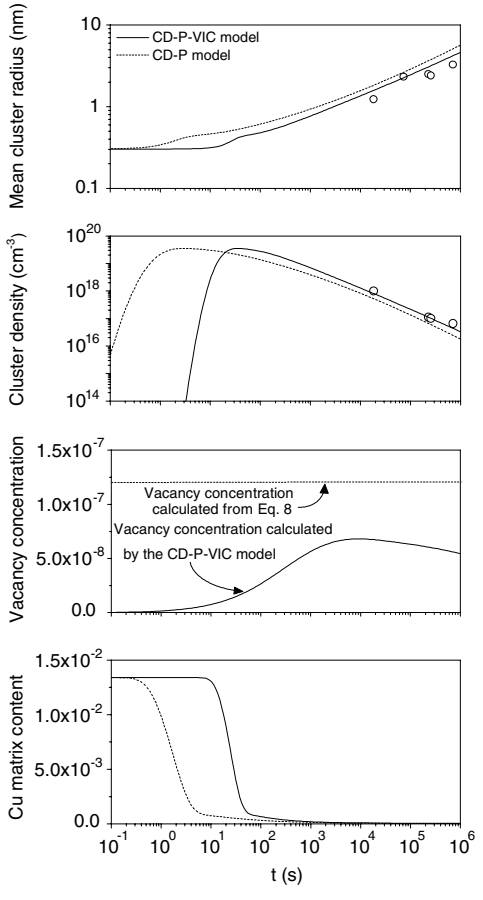

Fig. 7. Comparison between the CD-P model applied assuming a constant copper diffusivity and the CD-P-VIC model. Electron irradiation at 290 °C.

4. Copper precipitation during neutron irradiation

Copper precipitation under neutron irradiation was studied by Buswell et al. [11] using SANS in a Fe–1.3at.%Cu alloy at 290 °C. The dose rate used in that work was 5×10^{13} n cm^{-2} s^{-1}, which corresponds to 7.5×10^{-8} dpa s^{-1} according to the NRT approach [12]. Molecular dynamics calculations show that the NRT approach leads to an overestimation of the defect production rate: for iron, the defect production rate calculated by molecular dynamics is about 30% of the NRT rate [13], i.e. in this case 2.25×10^{-8} dpa s^{-1}.

Furthermore, contrary to electron irradiations, the primary damage does not consist only in point defects but also in point defect clusters [13]. The evolution of the production rate with the point defect cluster size was determined by molecular dynamics calculations for SIA and vacancies [14] and is shown in Fig. 8. Consequently, the production rate of isolated vacancies is 1.75×10^{-8} dpa s^{-1}, which corresponds to about 23% of the NRT rate. It should be noticed that the summation of the production rates corresponding to the different cluster sizes in Fig. 8 gives the production rate mentioned before: 2.25×10^{-8} dpa s^{-1}.

We used the same approach again as in the case of electron irradiation: considering a vacancy production rate of 1.75×10^{-8} dpa s^{-1}, the vacancy concentration was estimated in the permanent regime using Eq. (8). We found: $C_v = 3.5 \times 10^{-7}$. Then, the effective copper diffusivity under neutron irradiation at 290 °C was calculated using Eq. (9): $D^{irr} = 1.6 \times 10^{-13}$ cm^2 s^{-1}. This copper diffusivity value and the thermodynamic parameters of Eq. (2) were introduced in the CD-P model.

The CD-P-VIC model was also applied for neutron irradiation. As mentioned before, the main difference between neutron and electron irradiation is the nature of

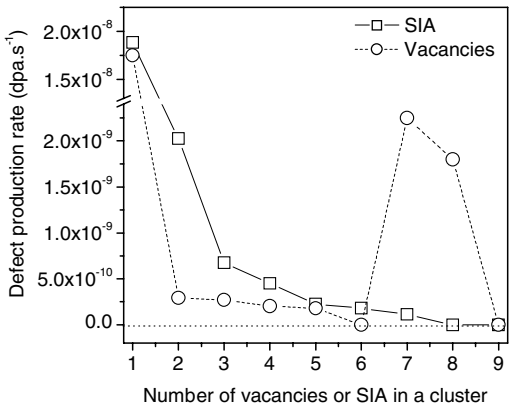

Fig. 8. Evolution of the point defect production rate with the point defect cluster size under neutron irradiation. Molecular dynamics calculations [14]. Notice the break in the production rate scale.

defects that are created in the material. For neutron irradiation, a production rate must be considered not only for vacancies and SIA but also for the smallest point defect clusters (Fig. 8). The other parameters introduced in the CD-P-VIC model for point defect clustering are the same as for electron irradiation (except G) and are listed in Table 1. Copper diffusivity was calculated at each time step in the CD-P-VIC model according to Eq. (9). Copper thermal diffusivity at 290 °C was calculated using Eq. (3) and the thermodynamic parameters given by Eq. (2) were used for copper precipitation.

The results of both models (CD-P model and CD-P-VIC model) are compared to the experimental data from Buswell et al. [11] in Fig. 9. It is shown that the CD-P-VIC model enables to fit the experimental data, which is not the case for the CD-P model assuming a constant copper diffusivity. Actually, analytical calculation of the vacancy concentration by Eq. (8) leads to a large overestimation in the case of neutron irradiation. That is why copper precipitation is much too fast according to the CD-P model.

5. Comment about copper diffusion by interstitial mechanism

In the calculations above, copper diffusivity under irradiation was deduced from Eq. (9) that is based on the assumption of copper diffusion by *vacancy* mechanism. Under irradiation, copper diffusion by *interstitial* mechanism should also be taken into account (for a detailed description of solute diffusion by interstitial mechanism, see for example Ref. [15]).

Eq. (11) gives an estimation of the effect of the interstitial mechanism on copper diffusivity [15]:

$$D^{\mathrm{irr}} \approx D^{\mathrm{th}} \frac{C_{\mathrm{v}}}{C_{\mathrm{v}}^{\mathrm{eq}}} + \alpha_{\mathrm{i}} D_{\mathrm{i}} C_{\mathrm{i}}, \tag{11}$$

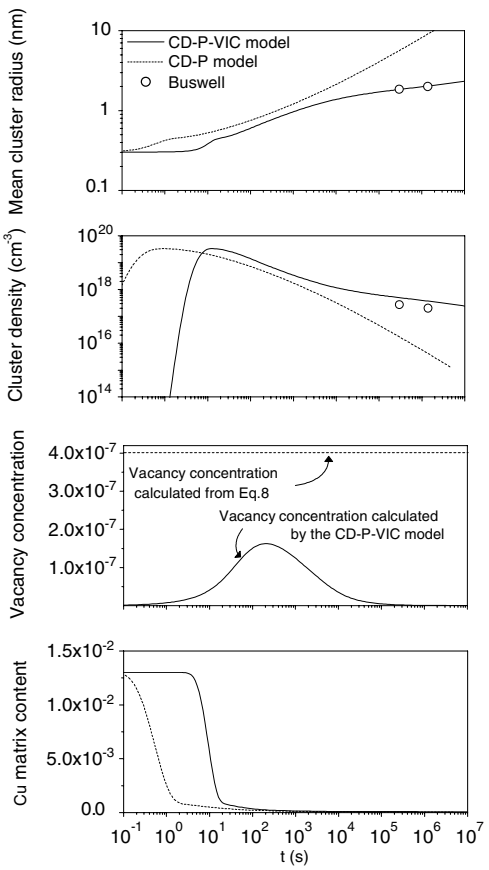

Fig. 9. Comparison between the CD-P model applied assuming a constant copper diffusivity and the CD-P-VIC model. Neutron irradiation at 290 °C.

where D_{i} is the SIA diffusivity, C_{i} is the SIA concentration during irradiation and α_{i} is an efficiency factor. As the size effect of copper in iron is relatively small, we will take $\alpha_{\mathrm{i}} = 1/2$, i.e. we will assume that copper does not modify the jump frequency of SIA [15].

From the evolution of C_{i} with time calculated by the CD-P-VIC model for electron and neutron irradiation, it can be shown that the $\alpha_{\mathrm{i}} D_{\mathrm{i}} C_{\mathrm{i}}$ term is negligible compared to the $D_{\mathrm{th}} \times C_{\mathrm{v}}/C_{\mathrm{v}}^{\mathrm{eq}}$ term, except for very little time of irradiation, where the SIA concentration is high ($t <$ 0.1 s). The CD-P-VIC model was applied using Eq. (11) and it was shown that taking copper diffusion by interstitial mechanism into account has no effect on the calculated curves of Figs. 7 and 9.

6. Conclusion

Modelling of copper precipitation in iron during thermal aging, electron irradiation and neutron irradiation was revisited in this paper. The main new conclusions can be stated as follows:

1. The CD-P model presented in [1] enables to describe copper precipitation in a Fe–1.34at.%Cu alloy at 500 °C assuming a copper diffusivity of 7.7×10^{-15} $cm^2\,s^{-1}$. Almost the same value is found applying the same model to copper precipitation in a Fe–1.1at.%Cu–1.4%Ni at 500 °C. The CD-P model was found to give almost the same results using the binding energy based on the classical capillary model or the one proposed by Golubov et al. [5].
2. The CD-P model was mixed to the CD-VIC model described in [6]. The CD-P-VIC model thus obtained enables to reproduce the experimental data for copper precipitation under electron and neutron irradiation [1,11] by taking into account the evolution of copper diffusivity with time during irradiation.

Acknowledgements

The authors would like to thank A.V. Barashev and S.I. Golubov for fruitful discussions.

References

[1] M.H. Mathon, A. Barbu, F. Dunstetter, F. Maury, N. Lorenzelli, C.H. de Novion, J. Nucl. Mater. 245 (1997) 224.
[2] M.K. Miller, K.F. Russell, P. Pareige, M.J. Starink, R.C. Thomson, Mater. Sci. Eng. A 250 (1998) 49.
[3] R. Kampmann, R. Wagner, in: C. Janot, W. Petry, D. Richter, T. Springer (Eds.), Atomic Transport and Defects in Metals by Neutron Scattering, Springer Proc. Phys. 10 (1986) 73.
[4] G. Salje, M. Feller-Kniepmeier, J. Appl. Phys. 48 (1977) 1833.
[5] S.I. Golubov, A. Serra, Yu.N. Osetsky, A.V. Barashev, J. Nucl. Mater. 277 (2000) 113.
[6] A. Hardouin Duparc, C. Moingeon, N. Smetniansky-de-Grande, A. Barbu, J. Nucl. Mater. 302 (2002) 143.
[7] J.W. Cahn, J.E. Hilliard, J. Chem. Phys. 28 (1958) 258.
[8] S.I. Golubov, A.V. Barashev, A.M. Ovcharenko, IPPE Report-9592, Ogninsk, 1997.
[9] M.S. Anand, R.P. Agarwala, J. Appl. Phys. 37 (1966) 4248.
[10] F. Maury, A. Barbu, to be published.
[11] J.T. Buswell, C.A. English, M.G. Hetherington, W.J. Phythian, G.D.W. Smith, G.M. Vorall, in: Proceedings of the 14th International Symposium on Effects of Irradiation in Materials, Vol. 2, Andover, MA, USA, ASTM-STP 1046, 1988, p. 127.
[12] M.J. Norgett, M.T. Robinson, I.M. Torrens, Nucl. Eng. Des. 33 (1975) 50.
[13] D.J. Bacon, A.F. Calder, F. Gao, J. Nucl. Mater. 251 (1997) 1.
[14] S. Jumel, private communication.
[15] A. Barbu, A.B. Lidiard, Philos. Mag. A 74 (1996) 709.